Fracture initiation and size effect in V-notched structures under mixed mode loading

Pietro Cornetti[1,*], **Alberto Sapora**[1], **Alberto Carpinteri**[1]

[1] Department of Structural, Building and Geotechnical Engineering, Politecnico di Torino, Torino, 10124, Italy
* Corresponding author: pietro.cornetti@polito.it

Abstract In asserting structural safety it is of paramount importance to be able to evaluate the loading capacity of notched components, where stresses concentrate and can trigger cracks leading to a catastrophic failure or to a shortening of the assessed life of the structure. Restricting the analysis to brittle materials, we apply the Finite Fracture Mechanics criterion to address the problem of a V-notched structure subjected to a mixed-mode loading, i.e. we provide a way to determine the direction and the load at which a crack propagates from the notch tip and express the critical conditions in terms of the generalized stress intensity factors plus a suitable definition of the notch mode mixity. Weight functions of the stress intensity factors for V-notch emanated cracks available in the literature allow us to implement the fracture criterion proposed in an almost completely analytical manner: the determination of the critical load and the direction of crack growth is reduced to a minimization-under-constraint problem. We then highlight the size effect for a V-notched structure under mixed-mode loading and the differences between the structural behaviours of cracked and notched geometries.

Keywords sharp notches, mode mixity, size effect, finite fracture mechanics

1. Introduction

The development of suitable fracture criteria for brittle (isotropic or orthotropic) materials containing V-notches or multi-material interfaces is a problem of primary concern in order to control fracture onset phenomena taking place in mechanical components, composite materials and electronic devices. As well-known, the singularity of the stress field in the vicinity of the notch tip makes the problem non-trivial.

Concerning re-entrant corners in homogeneous media subjected to mode I loadings, since the pioneering paper by Carpinteri [1] a good correlation has been found between the critical value of the generalized stress intensity factor (i.e. the generalized fracture toughness) and the failure loads. Theoretical models to relate the generalized fracture toughness to material tensile strength, fracture toughness and re-entrant corner amplitude have been set by a number of researchers, e.g. [2-5].

Fewer contributions are available for what concerns mixed mode loading conditions [6-8]. Here we provide the generalization of the results obtained by Carpinteri et al. [5] to mixed mode problems. The proposed approach (as well as the ones previously cited) is based on the assumption that the region around the corner dominated by the singular stress field is large compared to intrinsic flaw sizes, inelastic zones or fracture process zone sizes. This hypothesis is the analogous of small-scale yielding in Linear Elastic Fracture Mechanics (LEFM).

While in LEFM there is a direct connection between the Stress Intensity Factors (SIFs) and the strain energy release rate (i.e. Irwin's relationship), this relation is missing in the case of notches, so that correlating fracture initiations with critical values of the stress intensity [1] could appear questionable. However, the recently introduced Finite Fracture Mechanics (FFM) criterion has shown this is not the case [4,5]. In fact, under the assumption of a finite crack extension at fracture initiation, it is possible to prove a relation between the Generalized Stress Intensity Factors (GSIFs) and the energy released when a crack appears at the V-notch tip.

2. Stress intensity factors for a V-notch emanated crack

Let us consider a re-entrant corner in an infinite homogeneous elastic medium with a polar coordinate system (r,ϑ) centred at the V-notch tip (see Fig.1a). After Williams, the asymptotical stress field is given by:

$$\sigma_{rr} = \frac{K_I^*}{(2\pi r)^{1-\lambda_I}} f_{rr}^{I}(\vartheta,\omega) + \frac{K_{II}^*}{(2\pi r)^{1-\lambda_{II}}} f_{rr}^{II}(\vartheta,\omega) \tag{1a}$$

$$\sigma_{\vartheta\vartheta} = \frac{K_I^*}{(2\pi r)^{1-\lambda_I}} f_{\vartheta\vartheta}^{I}(\vartheta,\omega) + \frac{K_{II}^*}{(2\pi r)^{1-\lambda_{II}}} f_{\vartheta\vartheta}^{II}(\vartheta,\omega) \tag{1b}$$

$$\tau_{r\vartheta} = \frac{K_I^*}{(2\pi r)^{1-\lambda_I}} f_{r\vartheta}^{I}(\vartheta,\omega) + \frac{K_{II}^*}{(2\pi r)^{1-\lambda_{II}}} f_{r\vartheta}^{II}(\vartheta,\omega) \tag{1c}$$

where K_I^* and K_{II}^* are the GSIFs in mode I (symmetrical) and mode II (anti-symmetrical) loading conditions respectively, λ_I and λ_{II} are the well-known Williams' eigenvalues and the functions f_{ij} are the angular shape functions (i.e. the eigenvectors). Both eigenvalues and eigenvectors depend on the notch opening angle ω. Note that the definition of the GSIFs is somewhat arbitrary, depending on the choice of the normalization factor, here taken equal to $(2\pi)^{1-\lambda_i}$ as in [2] but equal to 1 or to $\sqrt{2\pi}$ in other papers (e.g. [7] and [3], respectively). As we shall see later, the advantage of such a choice is that the critical value of the mode I GSIF continuously varies from the material tensile strength to the material fracture toughness as the re-entrant corner amplitude diminishes from 180° (flat edge) to 0° (cracked plate).

In order to apply the FFM criterion, we need to evaluate the energy necessary for the abrupt appearance of a finite length crack at the notch tip. This quantity can be easily computed if the SIFs K_I and K_{II} of a crack at the notch vertex are known. To this aim, we begin noticing that, if the crack occurs within the GSIFs dominated stress field, the SIFs depend only on the GSIFs, crack direction ϑ, crack length a and notch opening angle ω (see Fig.1b). A straightforward application of the Π-theorem (as well as the principle of effect superposition) shows that this dependency must take the following form [9]:

$$K_I = \mu_{11}(\vartheta,\omega)\, K_I^* a^{\lambda_I - 1/2} + \mu_{12}(\vartheta,\omega)\, K_{II}^* a^{\lambda_{II} - 1/2} \tag{2a}$$

$$K_{II} = \mu_{21}(\vartheta,\omega)\, K_I^* a^{\lambda_I - 1/2} + \mu_{22}(\vartheta,\omega)\, K_{II}^* a^{\lambda_{II} - 1/2} \tag{2b}$$

In case of pure mode I loaded V-notches, the emanated crack grows along the notch bisector ($\vartheta = 0$); hence K_{II} is zero and K_I simplifies into [10]:

$$K_I = \mu_{11}(\omega) K_I^* \, a^{\lambda_I - 1/2} \tag{3}$$

While the dimensionless μ_{ij} parameters can be found tabulated with great accuracy for a crack, i.e. for $\omega = 0°$ [11], their values for a generic notch opening angle ω are not available. Nevertheless, they can be obtained by exploiting the results provided in [12], where the SIFs for a pair of forces per unit thickness (either normal or tangential) acting on the faces of a V-notch emanated crack are given. Beghini et al. [12] evaluated such SIFs for several ω and ϑ values by proper finite element computations and provided accurate analytical expressions of the SIFs. From such expressions and by the principle of effect superposition the coefficients μ_{ij} can be obtained analytically [13].

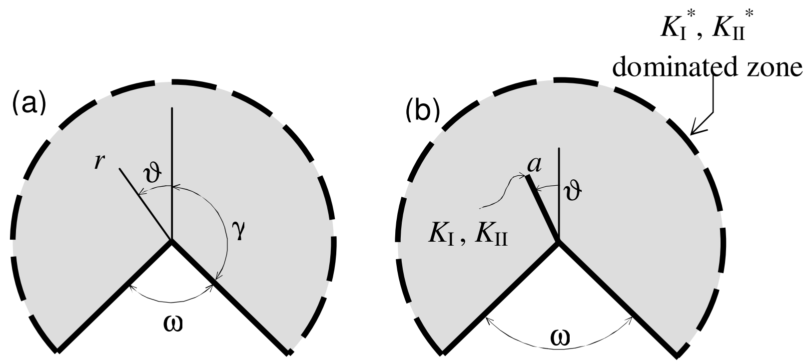

Figure 1. Polar reference system at the tip of a V-notch (a); V-notch emanated crack within the GSIFs dominated stress field region (b).

3. Coupled criterion

It is well known that both strength criteria and LEFM fail in predicting the failure load causing fracture propagation from a V-notch. In fact, the stress field given by eqn (1) is singular and strength criteria provide a vanishing failure load. On the other hand, the SIFs provided by eqn (2) vanish as the crack length *a* tends to zero and, consequently, LEFM provides an infinite failure load. These shortcomings can be overcome by resorting to Finite Fracture Mechanics [4,14], which couples the stress and energy approaches. Following the FFM approach proposed by Cornetti et al. [14], a crack propagates by a finite crack extension Δ if the following two inequalities are satisfied:

$$\begin{cases} \int_0^{\Delta} \mathcal{G}(a)\, \mathrm{d}a \geq \mathcal{G}_c\, \Delta \\ \int_0^{\Delta} \sigma_{\vartheta\vartheta}(r)\, \mathrm{d}r \geq \sigma_u\, \Delta \end{cases} \tag{4}$$

where σ_u is the material tensile strength and $\mathcal{G}_c$ is the fracture energy, related to the material fracture toughness by the well-known relation $\mathcal{G}_c = K_{Ic}^2 / E'$, where $E' = E / (1-\nu^2)$, E being the Young's modulus and ν the Poisson's coefficient.

The FFM criterion (4) can be regarded as a coupled Griffith-Rankine non-local failure criterion: the former inequality is an energy balance, whereas the latter is an (average) stress requirement for crack to propagate. It means that fracture is energy driven, but a sufficiently high stress field must act at the crack tip to trigger crack propagation. It is worth observing that, in the present case (which is the usual one, i.e. a positive geometry), the strain energy release rate function $\mathcal{G}(a)$ is monotonically increasing since the SIFs increase along with the crack length (see eqns (2)) while the stress $\sigma_{\vartheta\vartheta}(r)$ is monotonically decreasing with the distance r (see eqns (1)) from the notch tip (as far as both the modes provide a stress singularity, i.e. for a notch opening angle less than about 102.6°). This means that the lowest failure load (i.e. the actual one) is attained when the two inequalities are substituted by the two corresponding equations. In fact the first inequality is satisfied for crack steps larger than a threshold value, thus providing a lower bound for the set of admissible Δ-values; on the contrary, the second inequality is satisfied for crack advancements smaller than a certain value, thus providing an upper bound. For low load values, the upper bound is smaller than the lower bound and, consequently, the set of admissible Δ-values is empty. As the external load increases, the upper bound increases and the lower bound decreases till a load value is met (i.e. the failure load) for which both conditions are strictly fulfilled. Therefore, we conclude stating that the system (4) reverts to a system of two equations in two unknowns: the crack advancement Δ and the corresponding (minimum) failure load, represented by the values K_{If}^* and K_{IIf}^* of the GSIFs in critical conditions, implicitly embedded in the functions $\sigma_{\vartheta\vartheta}$ and $\mathcal{G}$. Exploiting the well-known Irwin's relationship in plane strain and mixed mode, the system (4) becomes:

$$\begin{cases} \int_0^{\Delta} [K_{\mathrm{I}}^2(a) + K_{\mathrm{II}}^2(a)]\, \mathrm{d}a = K_{\mathrm{Ic}}^2\, \Delta \\ \int_0^{\Delta} \sigma_{\vartheta\vartheta}(r)\, \mathrm{d}r = \sigma_{\mathrm{u}}\, \Delta \end{cases} \tag{5}$$

It is worth observing that the failure load estimate provided by the system (5) does depend on the crack propagation direction ϑ (see Fig.1b). Among all the possible directions, the actual one will be the direction ϑ_c providing the minimum failure load. Upon substitution of the SIFs eqns (2) into the first equation of the system (5) and integrating between 0 and Δ, we get:

$$\bar{\mu}_{11}\Delta^{2\lambda_{\mathrm{I}}}(K_{\mathrm{I}}^*)^2 + \bar{\mu}_{12}\Delta^{\lambda_{\mathrm{I}}+\lambda_{\mathrm{II}}}K_{\mathrm{I}}^*K_{\mathrm{II}}^* + \bar{\mu}_{22}\Delta^{2\lambda_{\mathrm{II}}}(K_{\mathrm{II}}^*)^2 = K_{\mathrm{Ic}}^2\Delta, \tag{6}$$

where, for the sake of simplicity, we have introduced the angular functions:

$$\bar{\mu}_{11} = \frac{\mu_{11}^2 + \mu_{21}^2}{2\lambda_{\mathrm{I}}}, \quad \bar{\mu}_{12} = 2\frac{\mu_{11}\mu_{12} + \mu_{21}\mu_{22}}{\lambda_{\mathrm{I}} + \lambda_{\mathrm{II}}}, \quad \bar{\mu}_{22} = \frac{\mu_{12}^2 + \mu_{22}^2}{2\lambda_{\mathrm{II}}} \tag{7}$$

Equation (6) highlights that the variation in the elastic energy is a quadratic function of the GSIFs. Equation (6) can be found also in Yosibash et al. [7], where it was derived in a different way, i.e. by directly computing coefficients of the quadratic form by suitable path independent integrals of the stress and displacement fields before and after the appearance of the finite crack advancement.

Upon substitution of the stress field represented by eqn (1) into the second equation of the system (5) and integrating between 0 and Δ, we get:

$$\bar{f}_{\vartheta\vartheta}^{\,\mathrm{I}}\, \Delta^{\lambda_{\mathrm{I}}} K_{\mathrm{I}}^* + \bar{f}_{\vartheta\vartheta}^{\,\mathrm{II}}\, \Delta^{\lambda_{\mathrm{II}}} K_{\mathrm{II}}^* = \sigma_{\mathrm{u}}\Delta \tag{8}$$

where, for the sake of simplicity, we have introduced the angular functions:

$$\bar{f}_{\vartheta\vartheta}^{\,\mathrm{I}} = \frac{f_{\vartheta\vartheta}^{\mathrm{I}}}{\lambda_{\mathrm{I}}(2\pi)^{1-\lambda_{\mathrm{I}}}}, \quad \bar{f}_{\vartheta\vartheta}^{\,\mathrm{II}} = \frac{f_{\vartheta\vartheta}^{\mathrm{II}}}{\lambda_{\mathrm{II}}(2\pi)^{1-\lambda_{\mathrm{II}}}} \tag{9}$$

4. Failure load, crack deflection and mode mixity

Under pure mode I loading condition, for symmetry reason the crack propagates along the notch bisector, i.e. $\vartheta_c = \vartheta_{\mathrm{Ic}} = 0$. Upon substitution of eqns (6) and (8), limited to the mode I contributions, into the system (5), we get:

$$\begin{cases} \bar{\mu}_{11}\Delta^{2\lambda_\mathrm{I}}(K_\mathrm{I}^*)^2 = K_\mathrm{Ic}^2\Delta \\ \bar{f}_{\vartheta\vartheta}^{\,\mathrm{I}}\,\Delta^{\lambda_\mathrm{I}}K_\mathrm{I}^* = \sigma_\mathrm{u}\Delta \end{cases} \tag{10}$$

The system (10) is readily solved, yielding the crack advancement Δ_c and the critical value K_{Ic}^* of the mode I GSIF K_I^* under pure mode I loading, i.e. the generalized fracture toughness [5]:

$$K_\mathrm{Ic}^* = \xi(\omega)\,K_\mathrm{Ic}^{2(1-\lambda_\mathrm{I})}\sigma_\mathrm{u}^{2\lambda_\mathrm{I}-1} = \xi(\omega)\,\sigma_\mathrm{u}\,l_\mathrm{ch}^{1-\lambda_\mathrm{I}}, \text{ with } \xi(\omega) = \lambda_\mathrm{I}^{\lambda_\mathrm{I}}\left[\frac{2(2\pi)^{2\lambda_\mathrm{I}-1}}{\mu_{11}^2(\vartheta=0,\omega)}\right]^{1-\lambda_\mathrm{I}} \tag{11}$$

where $l_{ch} = (K_{Ic} / \sigma_u)^2$ is the Irwin length. Note that, since ξ is equal to unity for ω equal to 0 or π, the generalized fracture toughness equals the fracture toughness for a cracked geometry and the tensile strength for a flat edge.

In the case of mixed mode loading, the critical values of the GSIFs can be obtained by substituting eqns (6) and (8) into the system (5):

$$\begin{cases} \left(\dfrac{K_\mathrm{I}^*}{K_\mathrm{Ic}^*}\right)^2 = \dfrac{\delta}{\xi^2\left(\bar{\mu}_{11}\delta^{2\lambda_\mathrm{I}} + \bar{\mu}_{12}\delta^{\lambda_\mathrm{I}+\lambda_\mathrm{II}}\tan\psi + \bar{\mu}_{22}\delta^{2\lambda_\mathrm{II}}\tan^2\psi\right)} \\ \dfrac{K_\mathrm{I}^*}{K_\mathrm{Ic}^*} = \dfrac{\delta}{\xi\left(\bar{f}_{\vartheta\vartheta}^{\,\mathrm{I}}\,\delta^{\lambda_\mathrm{I}} + \bar{f}_{\vartheta\vartheta}^{\,\mathrm{II}}\delta^{\lambda_\mathrm{II}}\tan\psi\right)} \end{cases} \tag{12}$$

where the mode I GSIF has been normalized with respect to the generalized fracture toughness K_{Ic}^*, the finite crack advancement with respect to l_{ch} ($\delta = \Delta / l_{ch}$) and ψ is the mode mixity, defined as:

$$\psi = \arctan\frac{K_\mathrm{II}^*\,l_\mathrm{ch}^{\lambda_\mathrm{II}-\lambda_\mathrm{I}}}{K_\mathrm{I}^*} \tag{13}$$

The system (12) can be recast as:

$$\begin{cases} \dfrac{K_\mathrm{I}^*}{K_\mathrm{Ic}^*} = \dfrac{\delta}{\xi\left(\bar{f}_{\vartheta\vartheta}^{\,\mathrm{I}}\,\delta^{\lambda_\mathrm{I}} + \bar{f}_{\vartheta\vartheta}^{\,\mathrm{II}}\delta^{\lambda_\mathrm{II}}\tan\psi\right)} \\ \delta - \dfrac{\left(\bar{f}_{\vartheta\vartheta}^{\,\mathrm{I}}\,\delta^{\lambda_\mathrm{I}} + \bar{f}_{\vartheta\vartheta}^{\,\mathrm{II}}\delta^{\lambda_\mathrm{II}}\tan\psi\right)^2}{\bar{\mu}_{11}\delta^{2\lambda_\mathrm{I}} + \bar{\mu}_{12}\delta^{\lambda_\mathrm{I}+\lambda_\mathrm{II}}\tan\psi + \bar{\mu}_{22}\delta^{2\lambda_\mathrm{II}}\tan^2\psi} = 0 \end{cases} \tag{14}$$

The technique of Lagrange multipliers can now be exploited to solve eqn (14). In fact, eqn (14) can be interpreted as a constrained minimization problem, since, once the geometry, material and loading are fixed (i.e. ω and ψ are given), the actual crack advancement Δ_c and crack orientation ϑ_c are the ones that minimize the first equation, i.e. the dimensionless failure load K_{If}^* / K_{Ic}^*, under the constraint represented by the second equation. Once the critical value K_{If}^* of the mode I GSIF is determined, the corresponding critical value K_{IIf}^* of the mode II GSIF is provided by eqn (13).

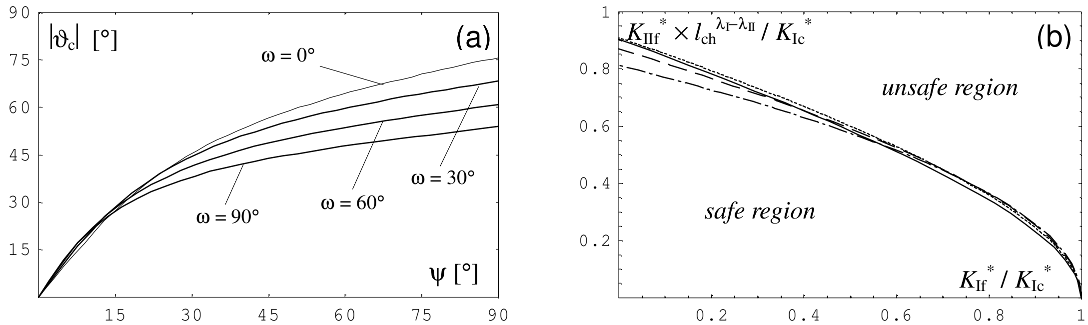

Figure 2. Crack deflection vs. mode mixity for different notch opening angle (a); safety domains in the GSIFs plane for different notch opening angles: continuous line, ω = 90°; dotted line, ω = 60°; dashed line, ω = 30°; dot-dashed line, ω = 0° (b).

The values of the crack orientation angle are plotted in Fig. 2a vs. the mode mixity ψ for different notch opening angle ω. On the other hand, the critical values of the GSIFs can be plotted in the (K_I^*, K_{II}^*) plane for a given notch opening angle ω and varying the mode mixity ψ. In this way we obtain a curve delimiting a safety region, i.e. points lying in this domain correspond to admissible stress states, whereas points lying outside correspond to failure. It is convenient to plot the results in a dimensionless form: the mode I GSIF is normalized with respect to the generalized fracture toughness K_{Ic}^*, whereas the mode II GSIF is normalized with respect to $K_{Ic}^* \times l_{ch}^{\lambda_I - \lambda_{II}}$. The safety domains are plotted in Fig. 2b for different ω values and in Fig. 3 for ω = 90°. If the external loads are increased proportionally, the ratio between the GSIFs keeps constant. It means that in the (K_I^*, K_{II}^*) plane, the loading curve is represented by a straight line starting from the origin. Furthermore, in the dimensionless plane, the angle between the loading path and the horizontal axis is exactly ψ.

According to the brittleness assumption, failure is attained suddenly when the straight line crosses the curve delimiting the safety domain, point A (Fig. 3). Apart from substitution of the SIFs with the GSIFs, this behaviour strictly resembles what occurs in the classical crack branching problem. Indeed, the crack branching problem is a particular case of the present one. However there is a substantial difference with respect to the crack kinking problem: if ω > 0°, the mode mixity ψ depends also on the material brittleness through l_{ch} (see eqn (13)) and not only on the loading, i.e. on the GSIFs ratio. For a given K_{II}^* / K_I^* ratio, the slope of the loading line will diminish for brittle materials (low l_{ch}), while will increase for less brittle materials (high l_{ch}): in other words, whatever is the GSIF ratio, the failure point migrates towards point B (pure mode I failure) as material brittleness increases, whereas it moves towards point C, if the brittleness decreases (within a certain range, otherwise, as explained in the following section, the asymptotic approach does not hold any more).

As clearly shown by eqn (13), the effect of the material on the mode mixity increases as the notch opening increase. In fact, for larger ω, the gap between the Williams eigenvalues λ_{II} and λ_I grows. On the other hand, for a vanishing notch opening angle, both λ_{II} and λ_I tend to 1/2 and the effect of the material vanishes. This material dependence is valid also for the orientation of the V-notch emanated crack, see Fig. 2a: as brittleness increases, l_{ch} diminishes, ψ diminishes and the crack deflection ϑ_c tends to zero, i.e. the V-notch emanated crack tends to propagate in mode I along the bisector. On the other hand, for less brittle material, the crack deflection is higher under the same GSIFs ratio. Once more, it is worth emphasizing the fundamental difference with respect to the crack case, where the angle of the crack kinking depends only on the (dimensionless) SIFs ratio, i.e. is the same independently of the material.

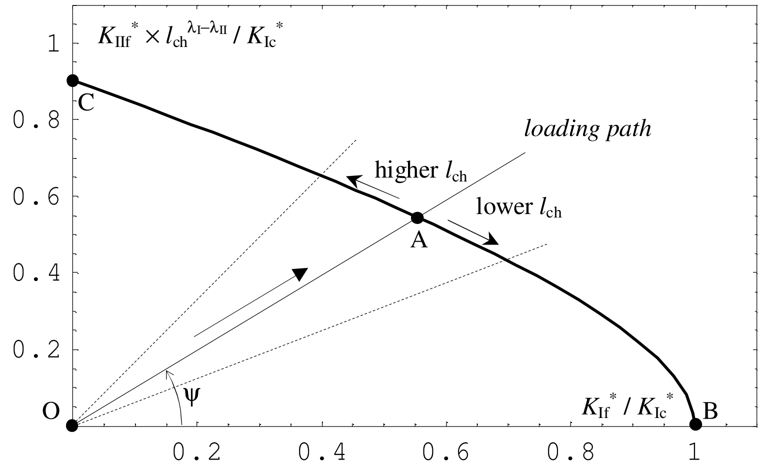

Figure 3. Resistance domain in the GSIFs plane (ω = 90°): points lying beneath the thick curve correspond to admissible stress states and vice-versa.

In Fig. 2b we plotted the safety domains for different notch opening angles ω. It is evident that all the curves are similar. Of course, this fact does not imply that the failure load does not vary with ω, since the physical dimensions as well as the shape functions defining the GSIFs vary along with ω. It simply shows that the transition from mode I to mode II fracture is approximately the same for all the notch amplitudes.

5. Size effect and mode mixity

The introduction of a physical length against which to scale the notch tip GSIFs enables further aspects of the solution to be drawn out, such as the influence of a V-notch on the so-called size effect. Hence let us consider a set of self-similar geometries as the ones drawn in Fig. 4. Dimensional analysis allows us to write directly:

$$K_{\mathrm{I}}^* = f_{\mathrm{I}}(\omega, a/b)\,\sigma\, b^{1-\lambda_{\mathrm{I}}}\,, \quad K_{\mathrm{II}}^* = f_{\mathrm{II}}(\omega, a/b)\,\sigma\, b^{1-\lambda_{\mathrm{II}}} \tag{15}$$

where σ is the nominal stress, b is a characteristic size of the structure and f_{I}, f_{II} are shape factors depending on the geometry, here synthetically defined by the notch opening angle ω and relative notch depth a/b.

Now let us focus our attention to the size effect on the nominal stress at failure σ_f. If only either the mode I or the mode II GSIF is different from zero, failure will occur whenever the corresponding GSIF reaches K_{Ic}^* or K_{IIc}^*, respectively (the latter value being given by the intercept with the vertical axis in Fig. 3). Hence, according to eqn (15), the logarithm of the nominal stress at failure is given by [1]:

$$\ln\sigma_{\mathrm{f}} = \ln\left[\frac{K_{\mathrm{Ic}}^*}{f_{\mathrm{I}}(\omega, a/b)}\right] - (1-\lambda_{\mathrm{I}})\ln b \qquad \text{or} \qquad \ln\sigma_{\mathrm{f}} = \ln\left[\frac{K_{\mathrm{IIc}}^*}{f_{\mathrm{II}}(\omega, a/b)}\right] - (1-\lambda_{\mathrm{II}})\ln b \tag{16}$$

It means that in a bi-logarithmic plot the strength vs. size curve is a straight line with (negative) slope equal to either $(1-\lambda_{\mathrm{I}})$ or $(1-\lambda_{\mathrm{II}})$, see Figs. 5a,b. Since $\lambda_{\mathrm{II}} > \lambda_{\mathrm{I}}$, the size effect is stronger under mode I than under mode II loadings.

On the other hand, in the case of mixed mode loadings, we have to substitute both eqns (15) into the stress condition (8) for crack propagation. Accordingly, we get:

$$\frac{\sigma_f}{\sigma_u} = \frac{1}{f_I(\omega, a/b)\left[\bar{f}^{\,I}_{\vartheta\vartheta}\big/\delta^{1-\lambda_I}\right] s^{-2(1-\lambda_I)} + f_{II}(\omega, a/b)\left[\bar{f}^{\,II}_{\vartheta\vartheta}\big/\delta^{1-\lambda_{II}}\right] s^{-2(1-\lambda_{II})}} \tag{17}$$

where we introduced the brittleness number s as [15]:

$$s = \frac{K_{Ic}}{\sigma_u \sqrt{b}} = \sqrt{\frac{l_{ch}}{b}} \tag{18}$$

The terms in square brackets in eqn (17) show a modest variation with the size, so that the terms in round brackets dominate. It means that, for large sizes and/or brittle materials, the first addend at the denominator (i.e. mode I) prevails; on the other hand, for small sizes and/or less brittle materials, the second addend at the denominator (i.e. mode II) does govern the problem. The presence of the brittleness number s in (17) highlights that the transition from mode I- to mode II-governed failure depends both on size and material brittleness. Thus we conclude that the size effect for a V-notched structure under mixed mode loading is represented by a curve with two slant asymptotes in the bilogarithmic plot (see Fig. 5c): the right one with slope $(1-\lambda_I)$, the left one with slope $(1-\lambda_{II})$. This is a general trend, i.e. independent of the geometry and fracture criterion adopted.

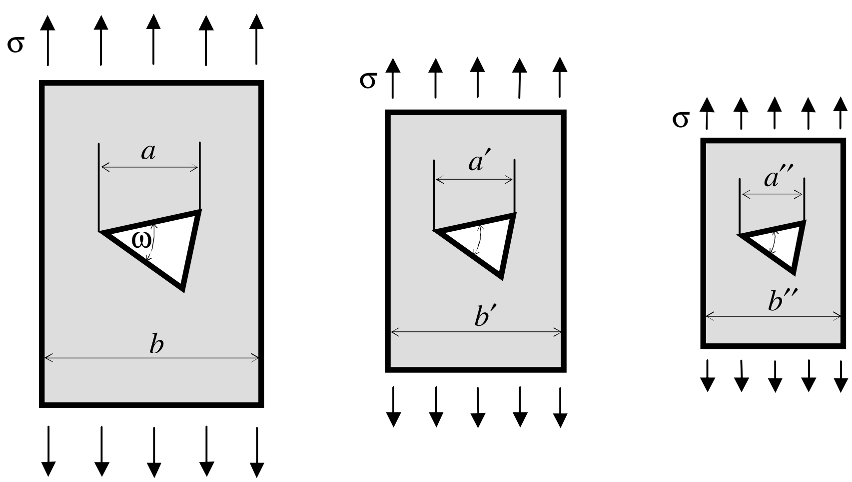

Figure 4. Self-similar specimens with a re-entrant corner of amplitude ω.

It is worth observing that the analysis of the mode mixity leads to the same conclusion. In fact substitution of eqns (15) into eqn (13) provides:

$$\psi = \arctan\left[\frac{f_{II}(\omega, a/b)}{f_I(\omega, a/b)} \quad s^{2(\lambda_{II}-\lambda_I)}\right] \tag{19}$$

Equation (19) clearly shows that, except in the crack case ($\lambda_I = \lambda_{II} = 1/2$), the mode mixity does not depend only on the shape factors, but also on the brittleness number, i.e. on the structural size. In fact, whatever is the ratio between f_{II} and f_I (provided they are both different from zero), for sufficiently large sizes the mode mixity will always tend to zero (i.e. pure mode I), whereas it will tend to $\pi/2$ for vanishing sizes (i.e. pure mode II).

While the large-size asymptote is always physically meaningful, the small-size asymptote could become only theoretical if mode II prevails for sizes too small for the asymptotic approach to hold true. In fact, when the finite crack extension is not negligible with respect to the other geometrical dimensions (e.g. for very small sizes), disregarding higher order terms in the asymptotic stress field is not acceptable. Similarly to LEFM, the asymptotic approach to V-notched structures leads to an infinite strength for vanishing sizes, i.e. to a result that, within the present coupled Rankine-Griffith criterion and under constant remote tensile stresses (see Fig. 4), must be regarded as physically unacceptable.

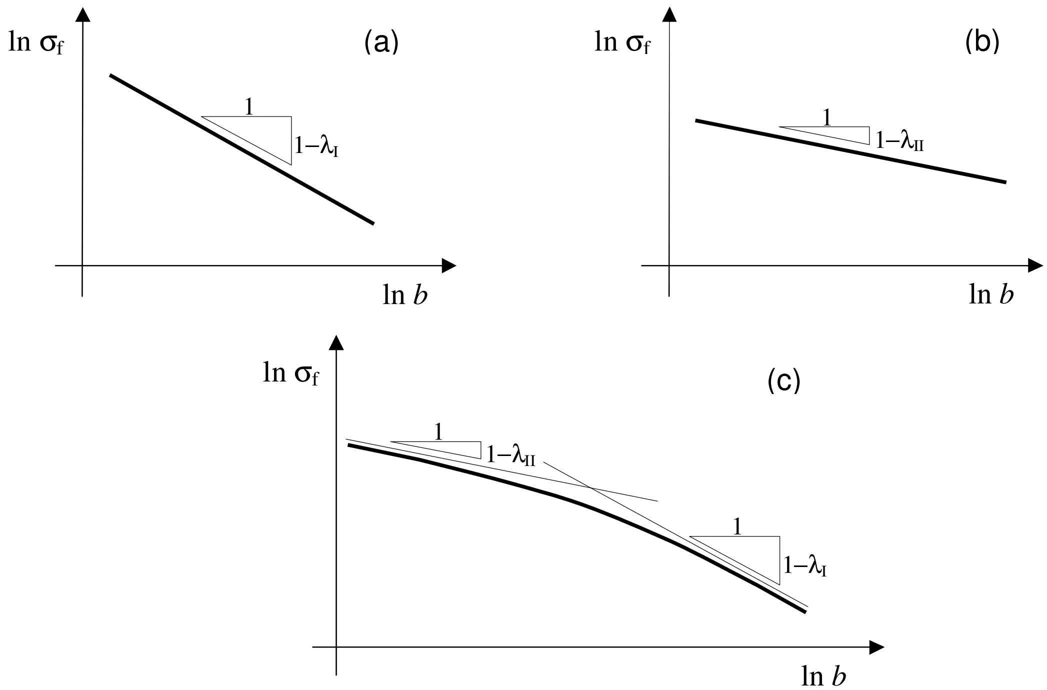

Figure 5. Size effect on nominal stress at failure: (a) pure mode I loading; (b) pure mode II loading; (c) mixed mode loading.

6. Conclusions

In the present paper we applied the FFM criterion provided in Cornetti et al. [14] to determine the critical load in V-notched structures under combined Mode I and Mode II loadings. With respect to simple Mode I loadings [5], the mixed mode problem is more complex since, beyond the failure load, also the direction of the crack onset at the re-entrant corner tip is unknown. Nevertheless, exploiting suitable weight functions for the SIFs of a V-notch-emanated crack [12], we were able to formulate the model as a standard minimization-under-constraint problem and to solve it by means of the Lagrange multiplier technique. A comparison with a broad set of experimental data (for both the failure load and the crack orientation) can be found in the recently published paper [16].

In mixed-mode loading cases, we showed that our model is able to explain the growing relevance of the mode II contribution for increasing material lengths l_{ch}, while it is negligible if l_{ch} tends to zero. Nevertheless, since the present approach is based on the asymptotic stress field, it yields accurate results only for sufficiently small l_{ch} values (with respect to the other geometrical dimensions). If this condition is not met, it is necessary to consider further terms in the stress field asymptotic expansions [17] or to tackle the problem numerically [18].

References

[1] A. Carpinteri, Stress-singularity and generalized fracture toughness at the vertex of re-entrant corners. Engineering Fracture Mechanics, 26 (1987) 143-155.
[2] A. Seweryn, Brittle fracture criterion for structures with sharp notches. Engineering Fracture Mechanics 47 (1994) 673-681.
[3] P. Lazzarin, R. Zambardi, A finite-volume-energy based approach to predict the static and fatigue behavior of components with sharp V-shaped notches. International Journal of Fracture 112 (2001) 275-298.
[4] D. Leguillon, Strength or toughness? A criterion for crack onset at a notch. European Journal of Mechanics A/Solids 21 (2002) 61-72.
[5] A. Carpinteri, P. Cornetti, N. Pugno, A. Sapora, D. Taylor, A finite fracture mechanics approach to structures with sharp V-notches. Engineering Fracture Mechanics 75 (2008) 1736-1752.
[6] A. Seweryn, S. Poskrobko, Z. Mroz, Brittle fracture in plane elements with sharp notches under mixed-mode loading. Journal of Engineering Mechanics-ASCE 123 (1997) 535-543.
[7] Z. Yosibash, E. Priel, D. Leguillon, A failure criterion for brittle elastic materials under mixed-mode loading. International Journal of Fracture 141 (2006) 291-312.
[8] F.J. Gómez, M. Elices, F. Berto, P. Lazzarin, Fracture of V-notched specimens under mixed mode (I + II) loading in brittle materials. International Journal of Fracture 159 (2009) 121-135.
[9] J. Li, X.B. Zhang, Crack initiation prediction for V-notches under mixed-mode loading in brittle materials. Journal of the Mechanics of Materials and Structures 1 (2006) 1385-1404.
[10] N. Hasebe, J. Iida, A crack originating from a triangular notch on a rim of a semi-infinite plate. Engineering Fracture Mechanics 10 (1978) 773-782.
[11] S. Melin, Accurate data for stress intensity factors at infinitesimal kinks. Journal of Applied Mechanics 61 (1994) 467-470.
[12] M. Beghini, L. Bertini, R. Di Lello, V. Fontanari, A general weight function for inclined cracks at sharp V-notches. Engineering Fracture Mechanics 74 (2007) 602-611.
[13] P. Cornetti, A. Sapora, A. Carpinteri, Mode mixity and size effect in V-notched structures. International Journal of Solids and Structures 50 (2013) 1562-1582.
[14] P. Cornetti, N. Pugno, A. Carpinteri, D. Taylor, Finite fracture mechanics: a coupled stress and energy failure criterion. Engineering Fracture Mechanics 73 (2006) 2021-2033.
[15] A. Carpinteri, Static and energetic fracture parameters for rocks and concrete. Materials and Structures 14 (1981) 151-162.
[16] A. Sapora, P. Cornetti, A. Carpinteri, A Finite Fracture Mechanics approach to V-notched elements subjected to mixed-mode loading. Engineering Fracture Mechanics 97 (2013) 216–226.
[17] C.Z. Cheng, Z.R. Niu, N. Recho, Effect of non-singular stress on the brittle fracture of V-notched structure. International Journal of Fracture 174 (2012) 127-138.
[18] J. Hebel, R. Dieringer, W. Becker. Modelling brittle crack formation at geometrical and material discontinuities using a finite fracture mechanics approach. Engineering Fracture Mechanics 77 (2010) 3558-3572.